Breathlessness-related brain activation: electroencephalogram dipole modeling analysis

Taketoshi Seino[1, 2)], Yuri Masaoka[1)], Katsunori Inagaki[2)], Masahiko Izumizaki[1)]

1) Department of Physiology, Showa University School of Medicine

2) Department of Orthopaedic Surgery, Showa University School of Medicine

Contact to Dr. Masahiko Izumizaki

Department of Physiology, Showa University School of Medicine

1-5-8 Hatanodai, Shinagawaku, Tokyo 142-8555, Japan

Tel: +81 3 3784 8113

Fax: +81 3 3784 0200

Running title: Breathlessness-related brain activation

Abstract

Dyspnea is the feeling of a shortness of breath and is a major symptom of cardio-pulmonary disease. The symptoms of dyspnea include sensations such as labored respiration, chest tightness, air hunger, and uncomfortable or unpleasant urges to breathe. In this study, we investigated the brain areas associated with dyspnea using electroencephalogram dipole (EEG/DT) modeling. As EEG/DT recordings have good temporal resolutions, we assumed that we could find the neuroanatomical substrates of dyspnea in time course measures of inspiration. We measured EEG and respiration simultaneously during CO_2 rebreathing, which induced dyspnea in the subjects and allowed us to find inspiration-related potentials during dyspnea. The waveform of the potentials was composed of a negative peak at 100 ms and a positive peak at 250 ms, and the potentials referenced inspiration-related potentials during dyspnea. Our EEG/DT modeling showed that the left superior frontal and left orbitofrontal cortex (OFC)

were active during the 100 ms after inspiration onset. In the next 100 ms, the anterior cingulate cortex was activated, followed by the superior frontal and OFC. At 200 ms to 300 ms, dipoles finally converged in the left insula and amygdala. The first component of inspiration-related potentials involved frontal areas that play a role in the intention to inspire and emotional guidance. The late component incorporated areas related to emotional reaction. We suggest that dyspnea with increasing ventilation may involve intentions or efforts to continue inspiration activities, and consequently may associate the perception of dyspnea with unpleasant emotions.

Keywords: dyspnea, respiration, electroencephalogram dipole modeling, insula, amygdala

Introduction

Dyspnea is the feeling of shortness of breath and is a major symptom of cardio-pulmonary disease [1]. Dyspnea occurs not only in cardio-pulmonary disease, but also in anxiety and panic disorders. The symptoms of dyspnea include sensations such as labored respiration, chest tightness, air hunger, and uncomfortable or unpleasant urges to breathe. These feelings or the emotional sides of dyspnea are observed with air hunger, which has been regarded as an essential vegetative sensation, such as hunger or thirst. Air hunger is increased by afferent inputs such as, for example, CO_2 or hypoxia, which stimulate the respiratory chemoreceptors and increase air hunger [2]. Mechanoreceptor-based tidal inflation of the lungs relieves air hunger [3]. In addition to dyspnea as a vegetative sensation, the effort required for breathing is also one of the possible causes of breathlessness. Breathlessness increases in proportion to the sense of effort, with an increase of respiratory resistive load [4].

Recently, brain imaging techniques such as functional magnetic resonance imaging (fMRI) and position emotion tomography (PET) have reported cerebral representations during dyspnea in humans [5, 6]. Corfield et al [5] reported the limbic areas involved in dyspnea perception in a PET study. Banzett et al [6] found that strong activations of the anterior insular cortex was associated with laboratory-induced dyspnea. An fMRI study showed limbic and paralimbic loci of activation were within the anterior insula, anterior cingulate, operculum, cerebellum, amygdala, thalamus, and basal ganglia during air hunger [7]. Strengths of fMRI are that it has excellent spatial resolution and can identify anatomical localizations related to dyspnea. However, a limitation of fMRI is its lack of temporal resolution. Because dyspnea or air hunger may be associated with respiratory changes, we hypothesized that if CO_2 stimulation is applied through every inspiration, dyspnea would increase on a breath-by-breath basis. We aimed to study how each brain area is involved in the processing of inspiration activities during rebreathing of CO_2. A brain mapping technique with good

temporal resolution is electroencephalogram (EEG) dipole modeling analysis (EEG/DT). EEG/DT can detect the source generators of event-related potentials such as movement-related potentials [8] and auditory-related potentials [9].

Recently, we investigated olfactory-inspiration potentials, which are averaged potentials that are triggered at the onset of inspiration during olfactory stimuli [10]. As our data support the hypothesis that olfactory perception largely depends on inspiration, the olfactory-inspiration potentials at the onset of inspiration can be used as a trigger for EEG. Additionally, EEG/DT can estimate the source generators of this potential and detect olfactory processing related to inspiration onset with a good temporal resolution. The primary olfactory areas including amygdala (AMG), entorhinal cortex, hippocampus and orbitofrontal (OFC) were found as source generators of olfactory-inspiration potentials in accordance with inspiration onset [10].

By simultaneously recording EEG and respiration during CO_2 rebreathing,

which induces dyspnea, we have identified dyspnea-related inspiration potentials associated with source localization in EEG/DT.

Methods

Five normal subjects (all males; mean age 22.6 years) participated in this study. All subjects gave informed consent and the study was approved by the Ethics Committee of Showa University School of Medicine.

Experimental apparatus

The subjects were seated at rest in the laboratory room. A face mask with a transducer for measuring respiratory flow and volume with a flow meter was attached to each subject (CPX, Arco System, Chiba, Japan). The subjects rebreathed through a transducer from 6-L plastic bags containing a gas mixture of 5% carbon dioxide + 95% oxygen. Respiratory rate (RR),

tidal volume (V_T), minute ventilation ($\dot{V}_E$), and end tidal CO_2 concentration ($ETCO_2$) were continuously measured and the data recorded on a computer. We asked the subjects about their breathlessness by using a Borg scale [11] every 10 seconds.

Measurement of EEG and EEG/DT

Subjects were attached to 21 electrodes according to the International 10–20 system, with the reference electrode on the right earlobe. An EEG and electro-oculogram were recorded and stored in a digital EEG analyzer (DAE-2100, Nihon Kohden, Tokyo, Japan). The EEG was sampled at 200 Hz through a 0.016- to 30-Hz bandpass filter. Impedances were kept below 10 KΩ. Signals of the onset of odor stimulation and respiratory flow (described later) were obtained simultaneously by the EEG and oculogram recordings and stored in the EEG analyzer. After electrodes were attached, the subject was moved to a shielded room and seated on a chair.

Respiratory flow data obtained with the respiratory monitor were also stored in the EEG analyzer. Inspiration flows downward from a 0 level, and expiration flows upward. The onset of inspiration (0 level) was used as a trigger for collection of the averaging potentials.

To determine the generators of the averaged potentials, EEG/DT data was localized with a scalp-skull-brain head model, created with the Montreal Neurological Institute (MNI) standard coordinate system. EEG/DT involves calculation of the location of source generators in the brain from the electroencephalographic data. The actual potential field distribution recorded from the 19 scalp electrodes (V_{meas}) was compared with the calculated field distribution (V_{cal}) for an appropriately equivalent current dipole (for one-dipole estimations) or two appropriately equivalent dipoles (for two-dipole estimations). The inverse solution was used to determine the dipole location and orientation that best fit the recorded data [12]. The locations and vector moments of one- or two-current dipoles were iteratively changed within the head model until the minimal squared

difference between V_{meas} and V_{cal} was obtained by the simplex method [13]. Accuracy of location of generators estimated by a MNI standard head model was confirmed by comparison with those estimated with individually created head models [8]. In this study, we estimated the location of dipoles using both grand mean averaged potentials and individual averaged potentials with the MNI model. A detailed description of the dipole tracing method has been reported elsewhere [8, 9, 10].

Statistical analysis

For statistical analysis, a software package (SPSS, SPSS Japan) was employed. One-way repeated measures analysis of variance (ANOVA) was used to test for the effect of CO_2 on respiratory variables. RR, $\dot{V}_E$, V_T, ETCO2 and breathlessness during rest, CO_2 rebreathing and after CO_2 rebreathing (after) were compared with Bonferroni post-hoc multiple comparison.

The degree of source concentration can be calculated in terms of goodness of fit. A goodness of fit of 100% is ideal; however, in practice it is usually less than 100% owing to noise, electrode misalignment, or non-dipole components of the electric sources. In the present study, two dipoles estimated with a goodness of fit greater than 98% were considered to indicate a concentrated source.

Results

Respiratory variables and breathlessness scores

There was no difference in RR at baseline, during rebreathing of CO_2, and following rebreathing of CO_2 (P=0.22). V_T (P=0.02, Post-hoc, P<0.01) and $\dot{V}_E$ (P=0.007, Post-hoc, P=0.06) increased during CO_2 rebreathing. ETCO2 also increased during CO_2 rebreathing (P=0.001, post-hoc, P=0.001). There were significant changes in breathlessness measured with the Borg scale

($P<0.001$). Post-hoc testing showed a significant increase in CO_2 during CO_2 rebreathing ($P=0.001$) and after rebreathing ($P=0.005$) compared with the baseline period. There was a difference in breathlessness during CO_2 rebreathing and after CO_2 rebreathing ($P=0.005$).

EEG/DT results

Grand averages of the potentials triggered at inspiration onset during CO_2 rebreathing across the five subjects are shown in Figure 2 (top). The waveform of the potentials was composed of a negative peak at 100 ms and a positive peak at 250 ms. These potentials were referenced to inspiration-related potentials during dyspnea. The root mean square value (RMS) showed a slow negative slope from 0 to 200 ms and increased positively at 250 ms. Because the DT method detects moving dipoles over time after a triggering point (indicated as 0 in the Figure 1), we analyzed the dipole locations at each of the three components (0–100 ms, 100–200

ms, and 200–300 ms).

The number of dipoles from five subjects located in each anatomical region are shown in Table 1. Anatomical areas of interest related to dyspnea or air hunger were decided on based on previous PET and MRI studies [5,6,7]. Dipoles with a GOF of 98% or higher were considered significant. Specific regions during each time period are indicated as numbers with a shaded column. From 0–100 ms, dipoles converged in the left OFC and the left superior frontal cortex (L S frontal). The left anterior cingulate (A cingulate) was activated from 100 ms to 200 ms. Finally, the left insula and the left AMG were activated from 200 ms to 300 ms. Typical dipole localizations in sagittal and horizontal sections during each time period are shown in Figure 2 (bottom). Dipoles in sagittal sections corresponded to those in horizontal sections (some dipoles were show only in sagittal sections).

Discussion

In this study, we investigated the brain areas associated with dyspnea using EEG/DT modeling. As EEG/DT has good temporal resolution, we assumed that we could find anatomical brain regions related to dyspnea in the time courses of inspiration activities.

We confirmed that dyspnea was successfully induced by CO_2 rebreathing. As $ETCO_2$ increased during CO_2 rebreathing, V_T mainly contributed to the increase of $\dot{V}_E$, whereas the RR was unchanged. Hypercapnia and exercise increase ventilation and this increase of $\dot{V}_E$ comprises various combinations of V_T and RR. Initially, $\dot{V}_E$ increases V_T and there is a subsequent rapid increase in RR while V_T plateaus. Izumizaki et al. [14], suggested that V_T increases followed by RR increases during hypercapnia may be caused by dyspnea increases, the threshold of dyspnea occurrence and RR increases were similar.

As dyspnea causes negative emotions [15], the perception of dyspnea is

potentially associated with an increased respiratory rhythm during exposure to laboratory dyspnea-inducing stimuli. Negative emotions, such as anxiety, increase $\dot{V}_E$ with a marked increase in RR during rest [16]. Thus, respiratory output in combination with V_T and RR may produce a strong interaction between metabolic breathing and behavioral breathing. As observed in the responses during CO_2 breathing, only V_T contributed to $\dot{V}_E$ increases, suggesting that the dyspnea induced in this study may not be strong enough to cause transitions to RR increase.

This respiratory response during mild dyspnea may refer to brain activities investigated by EEG/DT. We found that the left superior frontal and left OFC were activated 100 ms after inspiration onset. During the next 100 ms, the anterior cingulate cortex was activated.

The superior frontal areas involved in motor planning and attention [17] and anterior cingulate play a role in motor planning and are regarded as premotor areas [8]. These areas of activations also were observed during movement-related potentials during voluntary motion [8]. On the one hand,

the OFC plays a role in guiding emotional guidance and shaping survival strategies [6]. From the observations of the first component of the inspiration-related potentials during dyspnea, we suggest that the intention or plan to initiate inspiration is related to activities in the superior frontal and anterior cingulate cortices, whereas evaluating emotional reactions is related to activity in the OFC.

These areas of activations suggest that intentions towards the next inspiration or effort to breathe may be involved. Between 200 and 300 ms, the dipoles finally converged in the left insula and amygdala. The insula is essential to the perception of dyspnea [6,7]. Electrophysiological and anatomical tracer investigations have provided evidence linking the insula to afferents and motor centers relevant to breathing. Afferents from respiratory chemoreceptors and pulmonary stretch receptors project to the granular and dysgranular insula, neighboring the principal activation [18]. Stimulation studies of the vagus and the insula have demonstrated reciprocal respiratory projections in man and other mammals [19].

The insula has efferent and afferent connections with all of the neighboring limbic and paralimbic structures including the operculum, anterior cingulate, orbital frontal cortex, thalamus, amygdala, and basal ganglia [6]. Reiman [20] proposed that the insula evaluates distressing stimuli carrying negative emotional valence. Dyspnea is a sensation that includes unpleasant affective responses, involving the perception of dyspnea [6]. Interestingly, around 300 ms, the amygdala was also activated. Amygdala activity is thought to involve anxiety, fear, and unpleasantness [21] and may be related to the aversive aspects of dyspnea. From these results, we propose that an emotional reaction can be recognized consciously as dyspnea at around 300 ms after inspiration onset.

As we noted earlier, increases of RR were not observed during CO_2 rebreathing in this study. It has been reported that anxiety increased RRs occur in parallel to increased amygdala activity [22]. Source generators of anxiety-related potentials triggered by inspiration onset during anxiety were found in the amygdala within 100 ms after inspiration onset. In this

study, AMG was found at 300 ms, which was already regarded as the time period for human recognition or perception. Therefore, in this study, anxiety-based increases in ventilation may be excluded, leaving purely dyspnea sensations during CO_2 rebreathing.

We could detect activations simultaneous to inspiration activities because of the high temporal resolution of EEG/DT. We showed the areas associated with dyspnea from intention for inspiration and emotional guidance in the frontal cortex, followed by emotional reactions to the recognition of dyspnea. Recognition of air hunger may depend on attention and anxiety levels and may also depend on personality traits. In future studies, it could be worth investigating whether increases of attention or anxiety may increase dyspnea or whether dyspnea differs between individuals. Dyspnea is a major symptom for patients with pulmonary and cardiovascular diseases and also psychological diseases, such as patients with hyperventilation or panic disorders. Our ultimate goal is to find a way

to reduce dyspnea using our new knowledge regarding its physiological and neurological aspects.

Figure legends

Figure 1

Respiratory variables at baseline, during CO_2 rebreathing, and after CO_2 rebreathing (after).

$P<0.05$, $P<0.01$*.

Figure 2

Grand mean averaged EEGs from 19 electrodes triggered by the onset of inspiration during CO_2 rebreathing. The upper panel shows the grand mean averaged EEG (inspiration-related potentials) across five subjects. The localization of typical dipoles are show in respect to inspiration onset (indicated as 0 ms). From 0 to 100 ms, the dipoles were converged in the left superior frontal cortex and left orbitofrontal cortex. From 100 to 200

ms, the dipoles were in the left cingulate cortex and finally in the left insula and amygdala over 200–300 ms. Dipoles with a goodness of fit of 98% or more were adapted.

References

(1) O'Donnell D, Banzett R, Carrieri-Kohlman V, et al. Pathophysiology of dyspnea in chronic obstructive pulmonary disease. Proceed of the American thoracic society.2007 ;Vol 4 :145-168.

(2) Banzett R, Lansing R, Reid M, et al. "Air hunger" arising from increased PCO mechanically ventilated quadriplegics. Re- spir Physiol. 1989 ;76: 53–67.

(3) Manning H, Shea S, Schw R,et al. Reduced tidal volume inreases "air hunger" at fixed PCO2 in ventilated quadriplegics. Respir Physiol . 1992;90: 19-30.

(4) Killian K, Gandevia S, Summers E, et al. : Effect of increased lung volume on perception of breathlessness, effort, and tension. J Appl.

Physiol . 1984;57 : 686-691.

(5) Corfield D, Fink G, Ramsay S, et al. Evidence for limbic system activation during CO2-stimulated breathing in man. J Physiol (Lond) . 1995;488:77–84.

(6) Banzett R, Mulnier H, Murphy K, et al. Breathlessness in humans activates insular cortex. Neuroreport. 2000; 11: 2117–2120.

(7) Evans K, Banzett R,L Adams L,et al .fMRI Identifies limbic, paralimbic, and cerebellar activation during dir hunger. J Neurophysiol. 2002;88: 1500–1511, 2001;10.1152/jn.00957.

(8) Inoue M, Masaoka Y, Kawamura M, et al: Differences in areas of human frontal medial wall activated by left and right motor execution: Dipole-tracing analysis of grand-averaged potentials incorporated with

MNI three-layer head model. Neurosci Lett. 2008;437 : 82-87.

(9) Koiwa N, Masaoka Y, Kusumi T et al. Sound localization difficulty affects early and late processing of auditory spatial information: investigation using the dipole tracing method. Clin Neurophysiol. 2010;121(9) : 1526-1539.

(10) Masaoka Y, Koiwa N,Homma I. Inspiratory phase-locked alpha oscillation in human olfaction : source generators estimated by a dipole tracing method. J Physiol. 2005;566 : 979-997.

11) Borg G. Psychophysical bases of perceived exertion. Med Sci Ports Exerc.1982;14:377-81.

12)He B, Musha T, Okamoto Y, et al. Electric dipole tracing in the brain by means of the boundary element method and its accuracy, IEEE Trans.

Biomed. Eng. 1987;34: 406-414 .

13) Kowalik J,Osborn M.Methods for unconstrained optimization problems.American Elsevier Publishing, New York, 1968.

14) Izumizaki M , Masaoka Y, Homma I. Coupling of dyspnea perception and tachypneic breathing during hypercapnia. Respiratory Physiology & Neurobiology. 2011;Volume 179, Issues 2–3, Pages 276–286.

15) Banzett R, Pedersen S, Schwartzstein R, et al. The affective dimension of laboratory dyspnea: air hunger is more unpleasant than work/effort Am. J. Respir. Crit. Care Med. 2008;177, pp 1384–1390.

16) Masaoka Y, Homma I : The effect of anticipatory anxiety on breathing and metabolism in humans. Respir Physiol 2001;128:171-177.

17) Mesulam M. Large-scale neurocognitive networks and distributed processing for attention, language and memory. Ann Neurol.1990; 28: 597–613.

18) Hanamori T, Kuntake T, Kato K, et al. Neurons in the posterior insular cortex are responsive to gustatory stimulation of the pharyngolarynx,baroreceptor and chemoreceptor stimulation, and tail pinch in rats. Brain Res Bull 1998;785: 97–106.

19) Kaada B. Somato-motor, autonomic and electrocorticographic responses to electrical stimulation of rhinencephalic and other structures in primates, cat and dog. Acta Physiol Scand.1951;24:1–285.

20) Reiman E. The application of positron emission tomography to the study of normal and pathologic emotions. J Clin Psychiatry.1997;58: 4–12.

21) Adolphs R, Tranel D, Damasio H,et al. Fear and the human amygdala. J Neurosci. 1995;15: 5879–5891.

22) Masaoka Y and Homma I.The source generator of respiratory-related anxiety potential in the human brain. Neurosci Lett.2000;283:21-24.

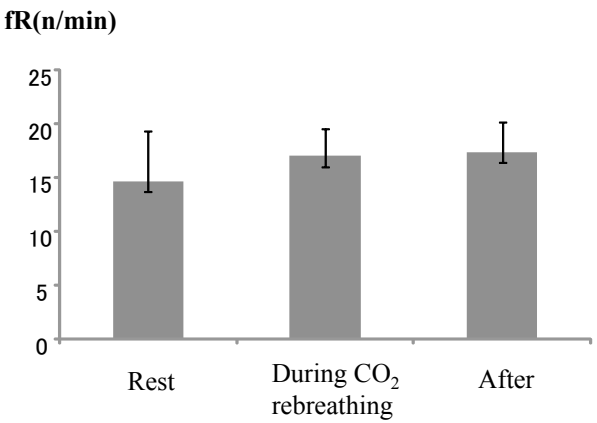
fR(n/min)
25
20
15
10
5
0
Rest
During CO_2 rebreathing
After

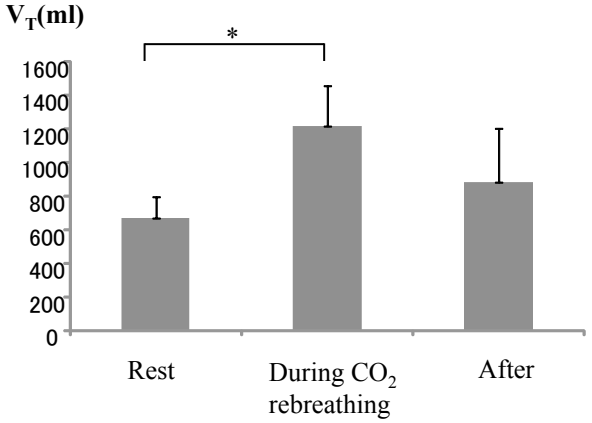
V_T(ml)
*
1600
1400
1200
1000
800
600
400
200
0
Rest
During CO_2 rebreathing
After

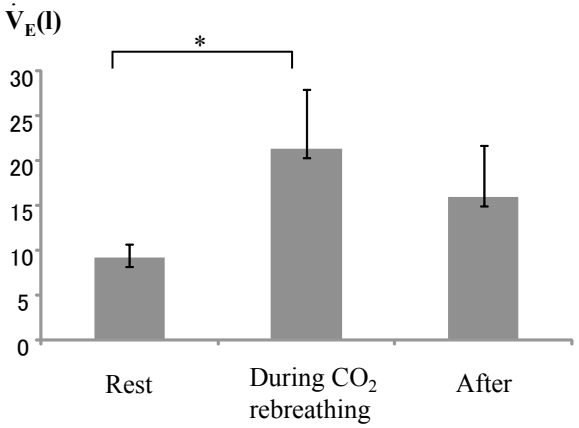
$\dot{V}_E$(l)
*
30
25
20
15
10
5
0
Rest
During CO_2 rebreathing
After

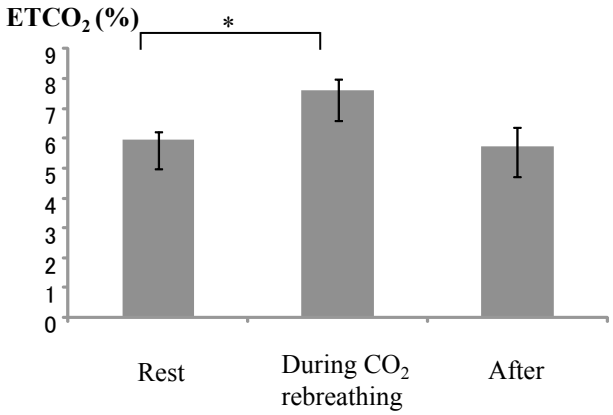
$ETCO_2$ (%)
*
9
8
7
6
5
4
3
2
1
0
Rest
During CO_2 rebreathing
After

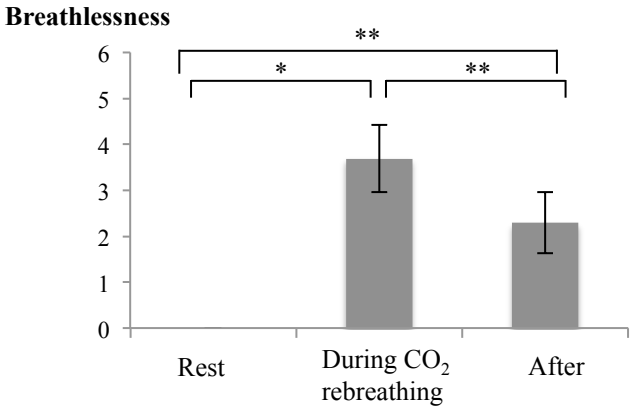
Breathlessness
**
*
**
6
5
4
3
2
1
0
Rest
During CO_2 rebreathing
After

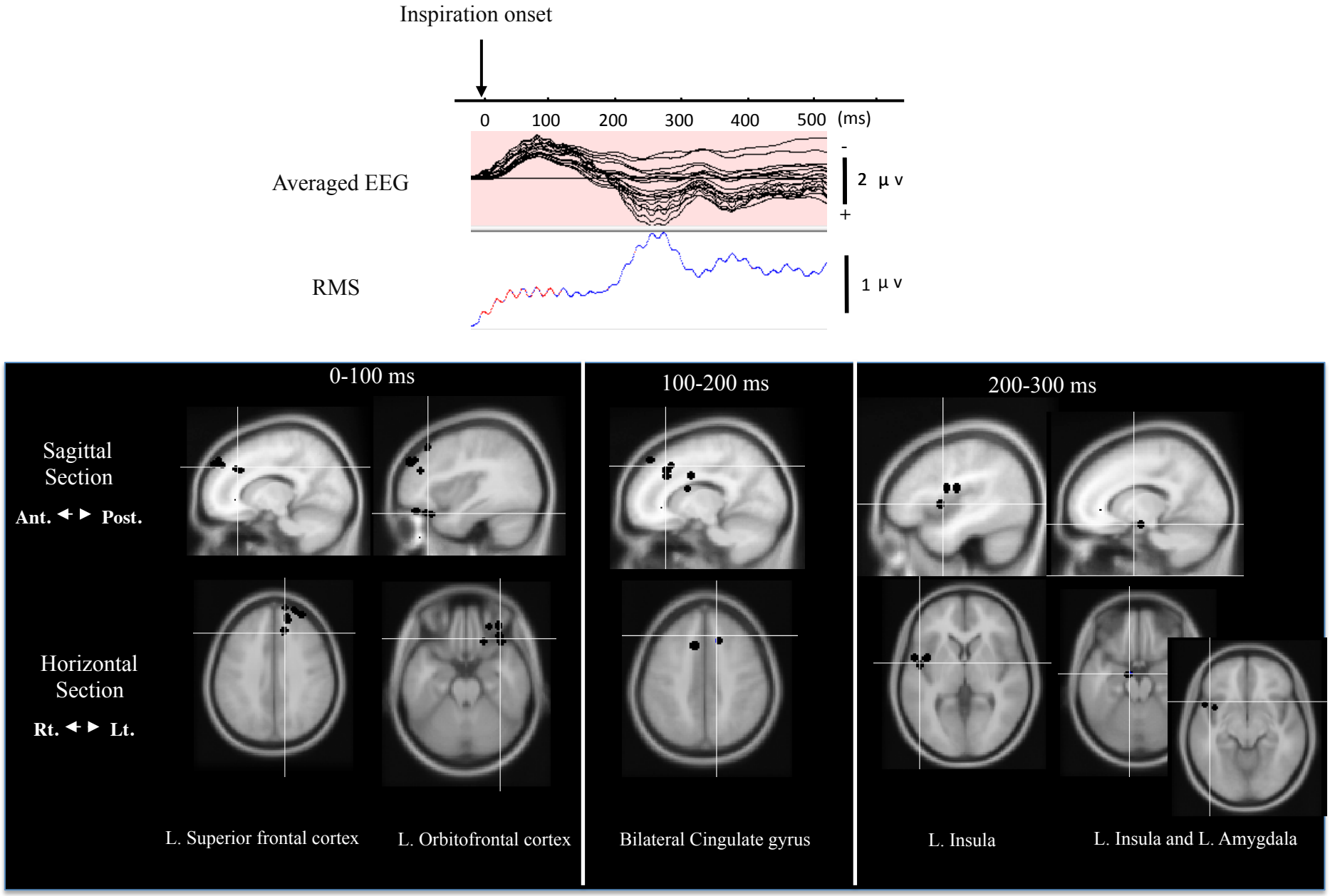
Inspiration onset
0
100
200
300
400
500
(ms)
Averaged EEG
-
2 μ v
+
RMS
1 μ v
0-100 ms
100-200 ms
200-300 ms
Sagittal Section
Ant. ◄ ► Post.
Horizontal Section
Rt. ◄ ► Lt.
L. Superior frontal cortex
L. Orbitofrontal cortex
Bilateral Cingulate gyrus
L. Insula
L. Insula and L. Amygdala

Table 1 Number of dipoles that converged by anatomical region

0 - 100 ms

Temporal lobe												Frontal lobe						Others			
Ins		ITG		MTG		STG		Para HC		AMG		OFC		S frontal		I frontal		A cingulate		M cingulate	
L	R	L	R	L	R	L	R	L	R	L	R	L	R	L	R	L	R	L	R	L	R
2	1	3	2	1	3	1	2	0	0	3	3	22	14	25	7	2	3	15	3	1	2

100 - 200 ms

Temporal lobe												Frontal lobe						Others			
Ins		ITG		MTG		STG		Para HC		AMG		OFC		S frontal		I frontal		A cingulate		M cingulate	
L	R	L	R	L	R	L	R	L	R	L	R	L	R	L	R	L	R	L	R	L	R
2	1	2	2	3	3	2	2	3	4	4	4	5	3	12	5	2	2	20	12	3	3

200 - 300 ms

Temporal lobe												Frontal lobe						Others			
Ins		ITG		MTG		STG		Para HC		AMG		OFC		S frontal		I frontal		A cingulate		M cingulate	
L	R	L	R	L	R	L	R	L	R	L	R	L	R	L	R	L	R	L	R	L	R
22	4	1	2	3	3	4	4	3	1	18	2	3	4	8	9	2	5	4	2	2	2

L=left, R=right
Ins, insula; ITG, inferior temporal gyrus; AMG, amygdala; MTG, middle temporal gyrus; STG, superior temporal gyrus;
Para HC, parahippocampal gyrus; AMG, amygdala; OFC, orbitofrontal cortex; S frontal, Superior frontal; I frontal, Inferior frontal;
A cingulate, Anterior cingulate cortex; M cingulate cortex, Middle cingulate cortex